

# Effect of input variability on the quality of laser shock processing<sup>†</sup>

Abul Fazal M. Arif\*

*Department of Mechanical Engineering, King Fahd University of Petroleum & Minerals, Dhahran, Saudi Arabia*

(Manuscript Received January 29, 2008; Revised March 17, 2009; Accepted May 9, 2009)

---

## Abstract

Laser shock processing (LSP) involves high-energy laser radiation combined with suitable overlays to generate high-pressure pulses on the surface of the metal. The stress wave generated due to high pressure pulses propagates into the material causing the surface layer to yield and plastically deform, and thereby, develop a significant residual compressive stress in the surface region of the substrate material. The developed compressive stress field is beneficial to improve surface properties such as fatigue, wear, and corrosion. To improve the understanding of the shock hardening process, investigation into the physical processes involved is necessary. In the first part of this paper, the temporal variation in the pressure intensity and spot size is calculated by using a two-dimensional recoil pressure prediction model. Using an explicit non-linear FEA code, ANSYS LS-DYNA, the deformation behavior and residual stresses in the substrate material are predicted. In the second part, a probabilistic approach to the modeling and analysis of LSP is presented in this paper. Various factors that affect the probabilistic performance of the LSP are grouped into categories and a select number of factors known to be significant, for which the variability could be assessed, are modeled as random variables (such as recoil pressure, laser beam spot size, substrate material properties and others). The potential of the probabilistic approach in predicting the structural integrity of the laser-shocked components is addressed.

*Keywords:* LSP; Shock peening; Shock waves; FEA; Residual stresses; Probabilistic model

---

## 1. Introduction

Laser-generated shock waves in a confining medium have been used to improve the mechanical properties in the surface region of various metals such as aluminum, steel and copper. In laser shock processing (LSP), the metallic surface to be treated is first locally coated with an overlay opaque to laser beam and then covered with a transparent overlay, a dielectric material transparent to laser beam (such as water or glass) as shown in Fig. 1. The opaque overlay acts as sacrificial material and a thin layer of it vaporizes on absorption of laser energy. An opaque overlay coating is used to protect the target from thermal effects so that nearly pure mechanical effects are in-

duced. The coating could be metallic foil, organic paints or adhesives. The transparent overlay confines the thermally expanding vapor and plasma against the surface of the target material, thus generating higher pressures than in the direct ablation mode. The resulting high pressure on the target induces a shock wave to propagate into the material. This shock wave is purely mechanical in nature and results in significant changes in the microstructure and properties. Pressures above 1 GPa are above the yield stress of most metals; thus plastic deformation can be induced and a compressive stress distribution in the irradiated volume can be formed [1].

Since the recoil pressure generated at the interface varies with time and space, due to the temporal and spatial distribution of the laser pulse, a study into effects of laser pulse on the laser induced shock characteristics becomes essential. Due to plastic deformation, LSP involves dents, which are due to shock

---

<sup>†</sup> This paper was recommended for publication in revised form by Associate Editor Jooho Choi

\*Corresponding author. Tel.: +966 3 860 2579, Fax.: +966 3 860 2949

E-mail address: afmarif@kfupm.edu.sa

© KSME & Springer 2009

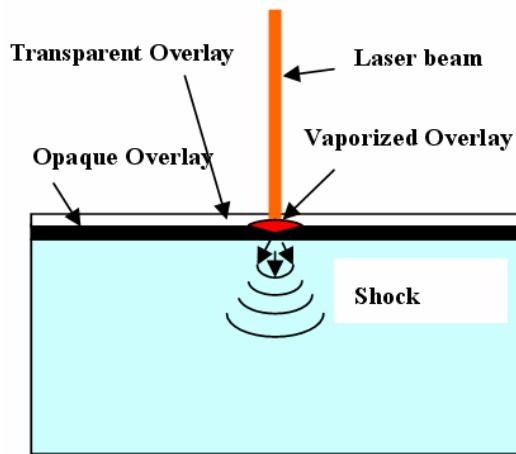


Fig. 1. Schematic of Laser-Shock Processing (LSP).

pressure without involving the thermal effects. Therefore, the possible quality measures for LSP include surface indentation depth, plastic strain and its depth, and the magnitude of the residual compressive radial stress. Considerable research studies on laser-shock processing were carried out previously [1-8]. However, most of these reported works are based on deterministic analysis. In the deterministic analysis, the model is expressed and described with a given set of specific numbers and values. Naturally, the results of such analysis are only as good as the assumptions and input values used for the analysis. However, in reality, every aspect of an analysis model is subjected to scatter. Results of the experimental investigations on the shock pressure during LSP also indicate scatter [3]. In addition, material property values are also different if one specimen is compared to the next. This kind of scatter is inherent for materials and varies among different material types and material properties. This means that most of the input parameters used in a finite element analysis of LSP are inexact, each associated with some degree of uncertainty and it highlights the importance of probabilistic analysis. The probabilistic analysis can be used to determine the effect of one or more variables on the outcome of the analysis.

The scope of this work is to identify and quantify the effects of various input parameters and their random nature on the mechanical behavior of the component after LSP. In the first part of this paper, the result of a shock pressure prediction model with varying interaction coefficient is presented. Using the predicted recoil pressure, the laser shock processing

of steel is investigated using deterministic nonlinear finite element analysis model. The results on axial displacement, plastic deformation and residual stresses are presented. In the second part, the probabilistic modeling of the LSP process is addressed and the results of the probabilistic analysis are presented.

## 2. Mathematical analysis

The mathematical analysis covers the prediction of recoil shock pressure and the shock wave analysis. The predictions of the shock pressure at the irradiated surface are used in the shock wave analysis to predict the elastic-plastic wave propagation in the irradiated region.

### 2.1 Shock pressure

Theoretical and experimental studies have provided a quantitative description of pressure environments that are generated at a metal surface by a pulsed laser beam. The important parameters governing the amplitude and shape of these pressures have been analyzed over a wide range of incident laser power densities and as a function of the type of target material and transparent overlay. In this paper, an analytical model presented by Fabbro et al. [6] has been numerically solved to estimate the pressure under different operating conditions. This model assumes that the laser irradiation is uniform and therefore shock propagation in the confining medium as well as in the target is one-dimensional. The governing equations during heating phase are [6]:

$$z \left( \frac{1}{2} + \frac{3}{4\alpha} \right) \frac{d^2 L(t)}{dt^2} + \frac{3z}{4\alpha} L(t) \frac{dL(t)}{dt} = \beta(t) I(t) \quad (1)$$

$$\frac{dL(t)}{dt} = \frac{2P(t)}{z} \quad (2)$$

where  $P(t)$  is the shock pressure,  $L(t)$  is the thickness of the plasma formed at the interface,  $I(t)$  is the incident laser intensity,  $\beta(t)$  is absorption coefficient and  $z = 2/(1/z_1 + 1/z_2)$  with  $z_1$  and  $z_2$  are the impedance of the target material and confining medium, respectively. This model considers the plasma as being a perfect gas with a corrective factor  $\alpha$  corresponding to the ratio of thermal to internal energy with  $\alpha = 1$  for a perfect gas.

Once the laser is switched off at time  $t = \tau$ , the plasma experiences an adiabatic cooling and the evolution of the uniform shock pressure can be described by the relation [6]:

$$P(t) = P(\tau) \left( 1 + \frac{(\gamma + 1)}{\tau} (t - \tau) \right)^{-\frac{\gamma}{\gamma + 1}} \tag{3}$$

The 1-D assumption is appropriate when the size of laser beam, which typically follows a Gaussian distribution, is relatively large [8]. The spatially uniform shock pressure  $P(t)$  relates to the spatially non-uniform distribution as:

$$P(r, t) = P(t) \exp\left(-\frac{r^2}{2r_0^2}\right) \tag{4}$$

where  $r$  is the radial distance from the center of the laser beam and  $r_0$  the radius of the laser beam. The above set of equations was solved numerically using appropriate initial values of  $P(t)$  and  $L(t)$ .

Fig. 2 shows a normalized laser-pulse profile with a full-width-at-half-maximum (FWHM) duration of 25 ns. Numerical simulations were conducted by using this kind of laser pulse, and the results were compared with experimental values reported by Berthe et al [3]. The input parameters used in the simulation are given in Table 1.

Table 1. Input parameters used in the simulation [3].

Wavelength	1064 ns
FWHM	25 ns
Shock impedance	Aluminum ( $z = 1.5 \times 10^6 \text{ kg/m}^2 \text{ s}$ ) Water ( $z = 1.65 \times 10^6 \text{ kg/m}^2 \text{ s}$ )

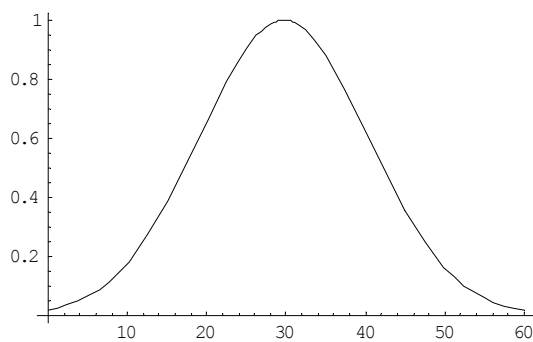


Fig. 2. A normalized Gaussian laser-pulse profile with a FWHM=25 ns.

Various researchers have used different constant values for the corrective factor  $\alpha$  [3]. However, it has been observed that its value varies with time before it becomes stable. In the current work, an effort has been made to develop a correlation for  $\alpha$  as a function of incident laser power density, as shown in Fig. 3(a), by using the measured data for maximum shock pressure reported by Berthe et al [3].

The peak pressure levels from the current simulation are reported in Fig. 3(b). It agrees very well with the experimental and simulation results reported in the literature [3, 9]. Dependence of shock pressure on laser intensity is shown in Fig. 4 where the laser power density varies from 1 to 10 GW/cm<sup>2</sup> for pulse duration of 50 ns.

**2.2 Residual stress analysis**

To investigate the effect of the elastic-plastic wave propagation on the deformation behavior and the distribution of stresses under varying laser energy

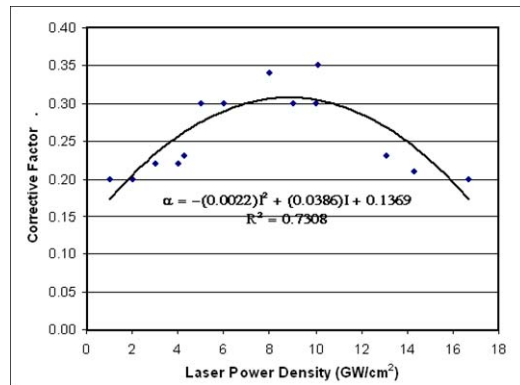


Fig. 3(a). Correlation for corrective factor ( $\alpha$ ).

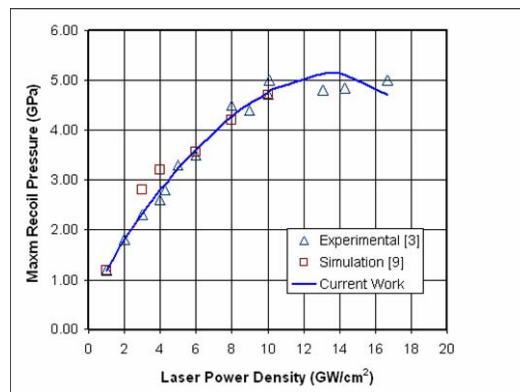


Fig. 3(b). Comparison of peak shock pressure.

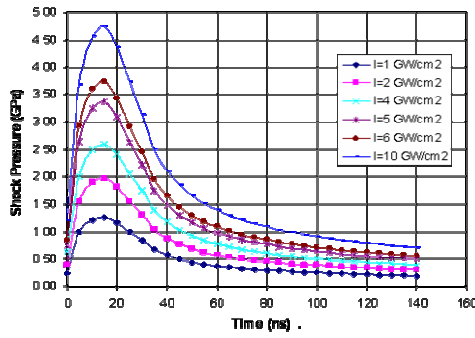


Fig. 4. Temporal variation of the shock pressure with varying laser power density.

density, a two-dimensional geometric model is needed. For this purpose, laser shock processing of a 5 mm thick steel plate was numerically simulated by using a commercial nonlinear explicit dynamic FE code ANSYS LS-DYNA [10]. For modeling purposes, only a circular piece of plate of 14 mm diameter was considered and two-dimensional axisymmetric finite element analysis was found to be adequate. To incorporate the temporal variation in the recoil pressure magnitude and size, the pressure predicted by Eq. (6) is used in this study at 4 GW/cm<sup>2</sup>. The time dependent pressure was applied on the top surface of the plate. The plate was meshed by PLANE162 element. PLANE162 is used for modeling 2-D solid structures in ANSYS LS-DYNA. The element can be used either as a planer or as an axisymmetric element.

The element is defined by four nodes having six degrees of freedom at each node: translations, velocities, and accelerations in the nodal x and y directions. The element is used in explicit dynamic analyses only. The FE model for the current study consists of 49296 elements and 50007 nodes.

Material behavior was idealized as strain rate dependent isotropic plasticity. In this model, a load curve is used to describe the initial yield strength,  $\sigma_0$ , as a function of effective strain rate. The yield stress for this material model is defined as:

$$\sigma_y = \sigma_0 \dot{\epsilon}' + E_h \epsilon_p^{eff} \tag{5}$$

where  $\sigma_0$  is the initial yield strength,  $\dot{\epsilon}'$  is the effective strain rate,  $\epsilon_p^{eff}$  is the effective plastic strain, and  $E_h$  is given by:

$$E_h = \frac{E E_{tan}}{E - E_{tan}} \tag{6}$$

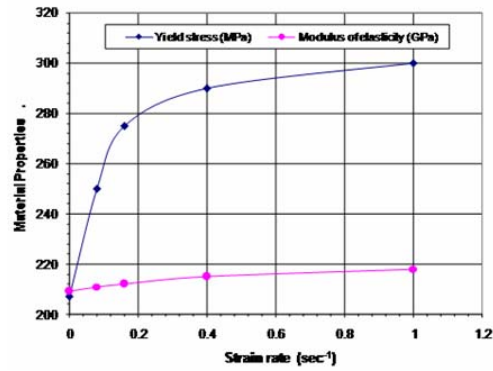


Fig. 5. Variation in yield stress and modulus of elasticity of steel with strain rate.

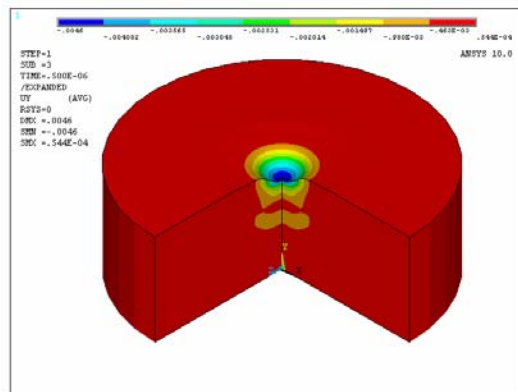


Fig. 6. Axial displacement (UY) at t=500 ns.

where  $E$  is the modulus of elasticity and  $E_{tan}$  is the tangent modulus for the material. The material properties used to model the constitutive behavior of the steel are  $E = 209$  GPa,  $\nu = 0.29$ , Density = 7802 kg/m<sup>3</sup>, and  $E_{tan} = 2.2$  MPa. The variation in the yield strength and the modulus of elasticity with strain rate is shown in Fig. 5.

Fig. 6 shows the axial displacement along the depth inside the substrate surface at 500 ns. In the early period surface displacement is reduced sharply as the depth increases towards the solid bulk. As the time progresses, the decay of axial displacement inside the substrate material becomes relatively gradual. Moreover, as the time progresses further reaching 500 ns, the axial displacement of the surface remains the same. Since the displacement has negative magnitude, the surface recesses towards the solid bulk. Consequently, recession becomes permanent indicating the plastic deformation in the substrate material. The high magnitude stress wave creates a plastic deformation

in the region of the substrate surface, in which case the depth of the deformed zone does not change with progressing time. The depth of the deformed zone extends on the order of 1.8 mm below the surface.

Fig. 7 shows the von Mises plastic strain contours for 500 ns duration. The displacement of the surface is towards the solid bulk of the substrate material due to plastic deformation of the surface. Consequently, a plastically deformed surface forms where the maximum surface recession is in the central region of the irradiated spot. However, the maximum magnitude of the plastic strain is at the surface in the order of 0.013.

Fig. 8 shows the residual stress contours developed in the deformed region, since the time 500 ns corresponds to well in excess of the laser pulse interaction time. The residual radial stress (SX) in the surface region is high, particularly in the central region of the irradiated spot and it is compressive due to plastic deformation of the surface. However, at some depth below the surface, the residual radial stress becomes tensile. The tensile residual stress component is associated with the plastic strain in this region. Consequently, a compressive stress wave front passing region after 500ns results in tensile residual stresses. Residual stress component extends in the radial direction, particularly in the surface region beyond the size of the irradiated spot radius. In the case of the axial stress component, the magnitude of the stress component is almost zero in the vicinity of the surface and as the depth below the surface increases (along the y-axis) towards the solid bulk, the stress component becomes first compressive and then tensile in the region of the symmetry axis. This behavior is due to the plastic strain developed in this region. When comparing the magnitude of the radial and the axial stresses, the radial stress is significantly higher than that of the axial stress. This is more pronounced in the surface region. Fig. 9 shows that the von Mises stress attains high values in the surface region, particularly in the vicinity of the surface. However, as the depth increases below the surface, it first decreases gradually and later sharply. The contribution of the radial stress component to the von Mises stress is dominant in the surface region of the workpiece. However, as the depth below the surface increases, the contribution of the axial stress component to the von Mises stress becomes equally important as the radial stress. However, its magnitude decreases and an elastic stress wave propagates in the substrate material with no further plastic deformation as shown in Fig. 9(b).

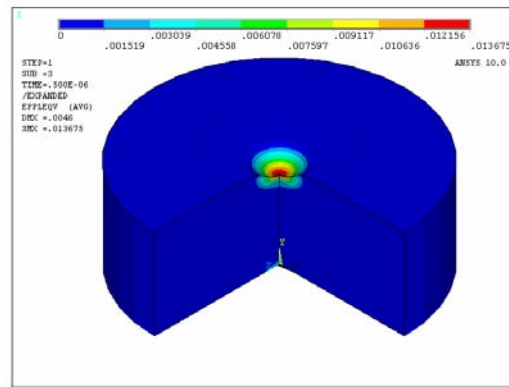


Fig. 7. von Mises plastic strain at t=500 ns.

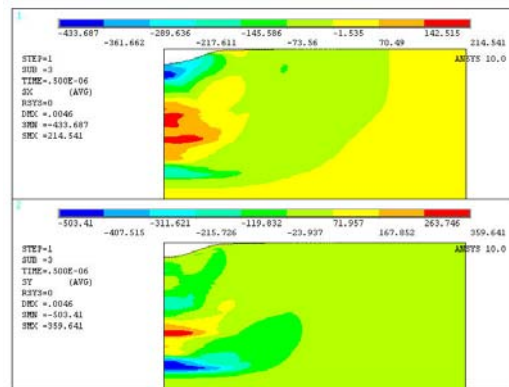
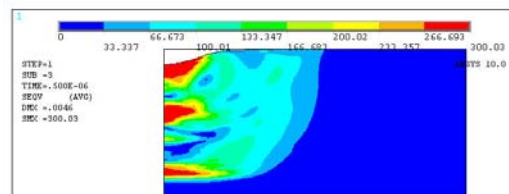
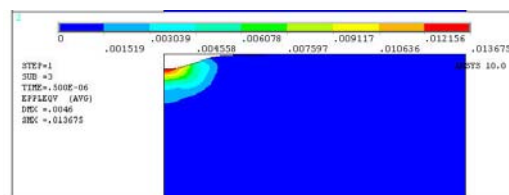


Fig. 8. Residual stress distribution at t=500ns; Radial Stress (Top), Axial Stress (Bottom).



(a)



(b)

Fig. 9. (a) Von Mises stress at t=500 ns; (b) Von Mises plastic strain at t=500 ns.

### 3. Probabilistic analysis

Considering the properties of the generated shock pressure or the material behavior realistically, it is necessary to take into account some uncertainty. This uncertainty can be conveniently described in terms of probability measures, such as statistical distribution functions. It is, therefore, the major goal of the current probabilistic analysis to relate the uncertainties of the input variables to the uncertainty of the structural performance of the substrate material. The output parameters considered in the current work are those important to measure quality of LSP process and it includes maximum axial deflection (DEFMAX), maximum von Mises plastic strain (EPLMAX) and maximum residual compressive radial stress (SXMAX). The deterministic model has 17 parameters that are regarded as random input variables. These variables characterize the uncertainty associated with the quality of the LSP in terms of the dents

Table 2. List of random input variables and their distribution ( $\mu$ = Nominal value,  $\sigma$ = standard deviation).

Variable		$\mu$	$\sigma$
$\sigma_y @ \dot{\epsilon}' < 0.08$ (MPa), YSTRESS1	Gaussian	207.0	$0.05 * \mu$
$\sigma_y @ \dot{\epsilon}' = 0.08$ (MPa), YSTRESS2	Gaussian	250.00	$0.05 * \mu$
$\sigma_y @ \dot{\epsilon}' = 0.16$ (MPa), YSTRESS3	Gaussian	275.0	$0.05 * \mu$
$\sigma_y @ \dot{\epsilon}' = 0.40$ (MPa), YSTRESS4	Gaussian	290.0	$0.05 * \mu$
$\sigma_y @ \dot{\epsilon}' = 1.0$ (MPa), YSTRESS5	Gaussian	300.0	$0.05 * \mu$
$\sigma_y @ \dot{\epsilon}' = 1.0$ (MPa), YSTRESS6	Gaussian	300.0	$0.05 * \mu$
Density (kg/mm <sup>3</sup> ), SDENSITY	Gaussian	$7.85E-6$	$0.05 * \mu$
$E @ \dot{\epsilon}' < 0.08$ (MPa), YOUNG1	Gaussian	$2.09E+5$	$0.05 * \mu$
$E @ \dot{\epsilon}' = 0.08$ (MPa), YOUNG2	Gaussian	$2.11E+5$	$0.05 * \mu$
$E @ \dot{\epsilon}' = 0.18$ (MPa), YOUNG3	Gaussian	$2.12E+5$	$0.05 * \mu$
$E @ \dot{\epsilon}' = 0.40$ (MPa), YOUNG4	Gaussian	$2.15E+5$	$0.05 * \mu$
$P(t) @ t=5$ ns (MPa), PMAX2	Lognormal	2000	$0.10 * \mu$
$P(t) @ t=5$ ns (MPa), PMAX3	Lognormal	2490	$0.10 * \mu$
$P(t) @ t=5$ ns (MPa), PMAX4	Lognormal	2600	$0.10 * \mu$
$P(t) @ t=5$ ns (MPa), PMAX5	Lognormal	2410	$0.10 * \mu$
$P(t) @ t=5$ ns (MPa), PMAX6	Lognormal	2060	$0.10 * \mu$
Laser beam spot size (mm), R0	Uniform	1.0	$\pm 0.05$

produced, compressive residual stress and plastic strain developed in the substrate material. A list of these random input variables, the distribution they are subjected to, and their distribution parameters are provided in Table 2.

During the probabilistic analysis using PDA module of ANSYS, 100 analysis loops were executed to compute the random output parameters as a function of the set of random input variables. The values for the input variables were generated randomly by Monte Carlo simulation to investigate how large the resulting scatter or uncertainty is that is induced on the output parameters due to random input variables. Which random input variables are contributing the most to the scatter of the random output parameters? Fig. 10 shows the variation and scatter in the output

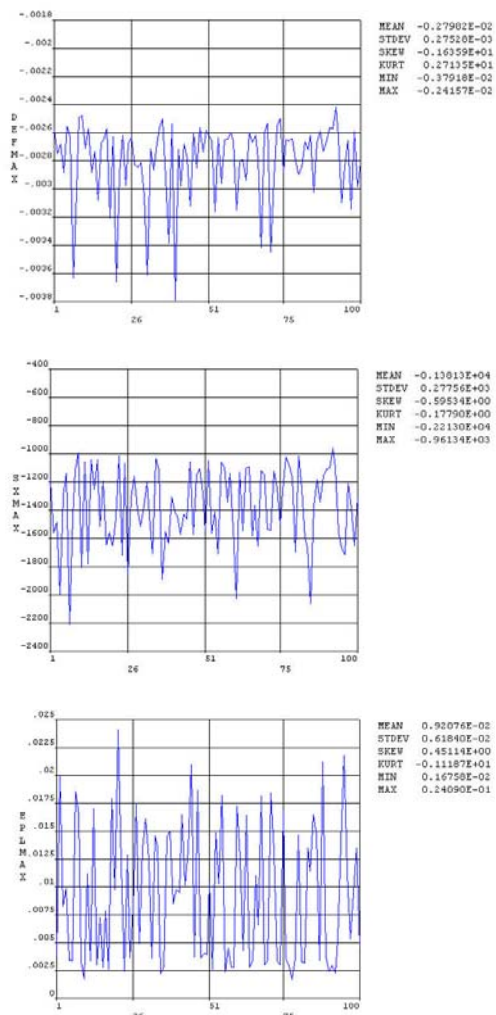


Fig. 10. Sample history of output quantities.

variables due to the random input variables. Statistics of the random output parameters calculated by the simulation are given in Table 3.

Sensitivity analysis is performed to find out which process parameters are the most critical to the performance of the LSP, and what are the critical ranges of those parameters. Fig. 11 shows a sensitivity plot indicating the most contributing random input variables for the scatter of the random output parameters.

Table 3. Statistics of random output parameters.

Name	Mean	Standard Deviation	Minimum	Maximum
DEFMAX	2.79E-3	2.75E-4	2.41E-3	3.79E-3
SXMAX	-1381	277.6	961.3	2213
EPLMAX	9.20E-3	6.18E-3	1.67E-3	2.40E-2

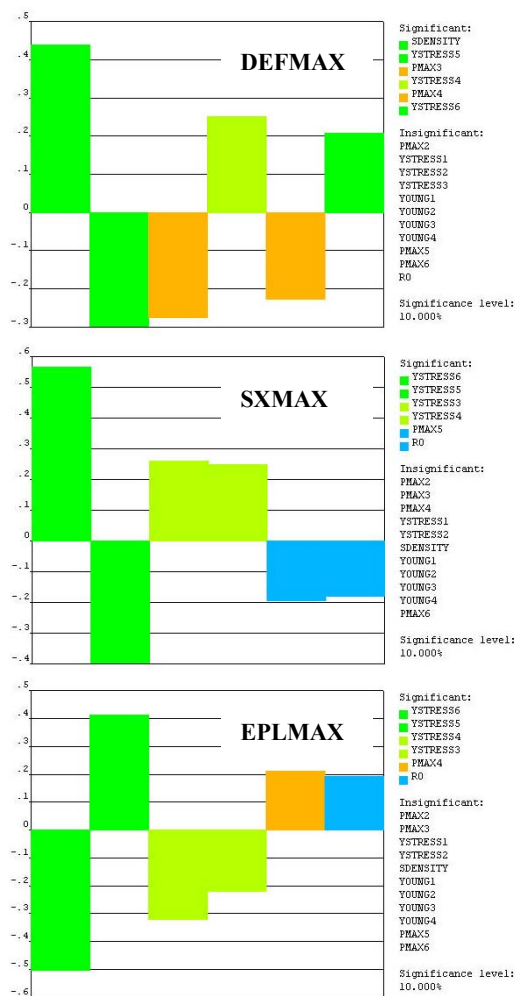


Fig. 11. Sensitivity plots of output parameters.

It is obvious from this figure that the material properties have the most significant effect on the randomness of all the three output variables. Substrate material density (SDENSITY) is the most important parameter for the dents produced due to LSP. The results show the strong dependence of the maximum compressive residual stress (SXMAX) and the maximum equivalent plastic strain (EPLMAX) on the yield strength variation especially at the strain rate of 1.0 or greater. As far as shock pressure is concerned, the peak pressure value (PMA4) is the most contributing followed by the laser beam spot size (R0).

Fig. 12 shows the scatter plots of the maximum residual radial stress (SXMAX) with respect to the yield strength at strain rate = 1.0 (YSTRESS5) and at strain rates greater than 1.0 (YSTRESS6). Scatter plots are a useful diagnostic tool for determining relationships or association between two variables. Such relationships manifest themselves by any non-random structure in the plot. A line of best fit has been drawn by using linear regression to study the correlation between the variables. Fig. 12(a) indicates a weak

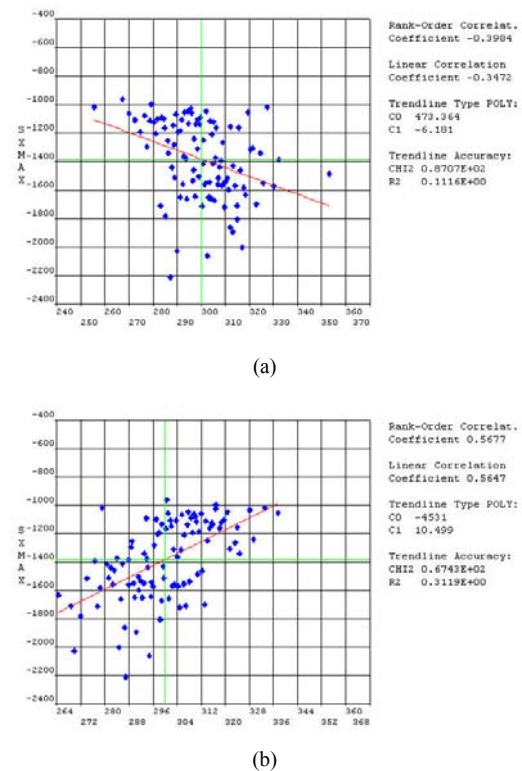


Fig. 12. Scatter plot of maximum residual radial stress (SXMAX) with respect to random input variables: (a) YSTRESS5 and (b) YSTRESS6.

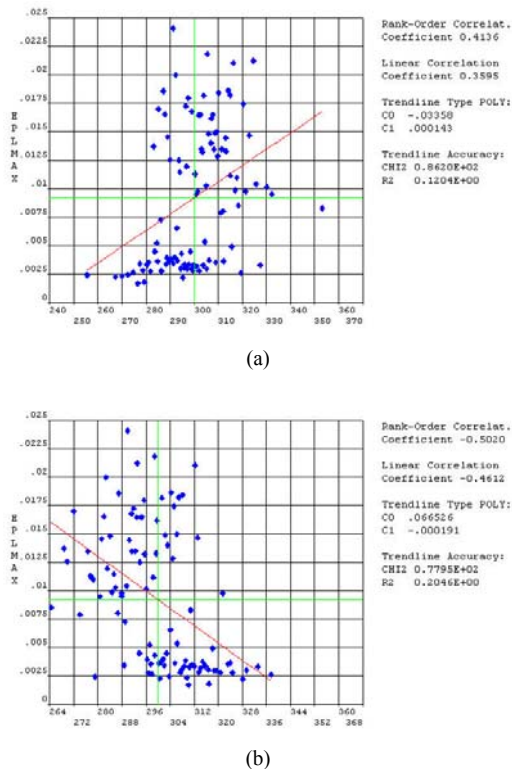


Fig. 13. Scatter plot of maximum equivalent plastic strain (EPLMAX) with respect to random input variables: (a) YSTRESS5 and (b) YSTRESS6.

negative correlation between SXMAX and YSTRESS5 having linear correlation coefficient = -0.3472, i.e., the slope of the line is negative with large scatter about the line. Whereas, SXMAX has a weak positive correlation with strength of substrate material at strain rate  $> 1.0$  (linear correlation coefficient = 0.5657) as shown in Fig. 12(b).

The scatter plots of the maximum equivalent plastic strain (EPLMAX) with respect to yield strength at two high strain rates are shown in Fig. 13. A linear correlation coefficient of 0.3595 for Fig. 13(a) indicates weak positive correlation between EPLMAX and YSTRESS5. Fig. 13(b) shows a weak negative correlation between EPLMAX and YSTRESS6 with linear correlation coefficient = -0.4612.

#### 4. Concluding remarks

A shock pressure prediction model based on the physics of the problem reported in the literature is numerically solved with a variable corrective factor to calculate nonuniform pressure distribution on the

surface. The effect of the temporal variation in the pressure intensity on the deformation behavior of steel is investigated by using an explicit nonlinear finite element program, and the residual stresses in the substrate material are calculated. It is found that the surface indentation is significantly large after the shock processing. The von Mises stress remains high in the vicinity of the surface after completion of the shock process and becomes larger towards the edge of the irradiated spot due to the plastic strain developed in this region.

The surface indentation, residual compressive radial stress and plastic strain have been identified as the important structural parameters for the determination of the quality of LSP process. A probabilistic approach to the LSP analysis is presented. The potential of this approach in predicting the actual variability of above parameters is clearly evident in the results. The analysis results show that the surface indentation produced and the compressive residual stress developed due to LSP are more sensitive to the variation of substrate material properties than the process parameters, such as recoil pressure and spot size. It is also found that the material properties and the process parameters have similar correlation with all the three important structural parameters.

#### Acknowledgment

The author acknowledges the support of King Fahd University of Petroleum & Minerals, Dhahran, Saudi Arabia for this work.

#### References

- [1] A. H. Clauer and H. J. Holbrook, Effects of Laser Induced Shock Waves on Metals, Shock Waves and High Strain Phenomena in *Metals-Concepts and Applications*, Plenum, New York, USA. (1981) 675–702.
- [2] A. F. M. Arif, Numerical prediction of plastic deformation and residual stresses induced by Laser Shock Processing, *J. of Materials Processing Technology*, 136 (2003) 120–138.
- [3] L. Berthe, R. Fabbro, P. Peyre, L. Tollier and E. Bartnicki, Shock waves from a water-confined laser-generated plasma, *J. Appl. Phys.*, 82 (6) (1997) 2826–2832.
- [4] B. S. Yilbas, A. F. M. Arif, S. Z. Shuja, M. A. Gondal and J. Shrikof, Investigation into Laser Shock



- Processing, *J. of Materials Engineering and Performance*, 13 (2004) 47-54.
- [5] B. S. Yilbas, A. F. M. Arif and M. A. Gondal, Plastic Deformation of Steel Surface Due to Laser Shock Processing, *Proc. Instn Mech Engrs Part B (Journal of Engineering Manufacture)*, 220 (2006) 857-867.
- [6] R. Fabbro, J. Fournier, P. Ballard, D. Devaux and J. Virmont, Physical Study of Laser-Produced Plasma in Confined Geometry, *J. Appl. Phys.*, 68 (1990) 775-784.
- [7] B. S. Yilbas and A. F. M. Arif, Laser Shock Processing of Aluminum: Model and Experimental Study, *Journal of Physics D: Applied Physics*, 40 (2007) 6740-6747.
- [8] W. Zhang and Y. L. Yao, Micro Scale Laser Shock Processing of Metallic Components, *ASME J. Mfg. Sc. and Engg.*, 124 (2002) 369-378.
- [9] B. Wu and Y. C. Shin, A self-closed thermal model for laser shock peening under the water confinement regime configuration and comparisons to experiments, *J. Appl. Phys.*, 97 (2005) 1-11.
- [10] ANSYS LS-DYNA User's Guide, ANSYS Inc., USA.



**Abul Fazal M. Arif** received his B.S. in Mechanical Engineering from NED University of Engg & Tech, Pakistan, in 1985. He then received his M.S. and Ph.D. degrees in Mechanical Engineering from the University of Minnesota, USA, in 1988 and 1991, respectively. He worked in the automobile industry for several years before joining academia in 1996 as a faculty member. He is currently an Associate Professor in Mechanical Engineering at King Fahd University of Petroleum & Minerals, Saudi Arabia. Dr. Arif's research interests lie in the areas of design and manufacturing. The fields of his research interest include Applied Mechanics, Modeling and Simulation of Manufacturing Processes, Finite Element Analysis and Laser applications in manufacturing. The efforts that Dr. Arif put in teaching and research have earned him several awards including the Donald Julius Groen Award from IMechE's Manufacturing Industries Division during Manufacturing Div. AGM on 13th September 2007.